Evaluating Deformation Corrections in Electrical Impedance Tomography

Alistair Boyle[1], William R.B. Lionheart[2], Camille Gómez-Laberge[1], Andy Adler[1]

[1]Systems and Computer Engineering, Carleton University, Ottawa, Canada
[2]School of Mathematics, University of Manchester, Manchester, UK

Abstract—**Electrical Impedance Tomography (EIT) uses the difference in measurements between surface electrodes to reconstruct an image of the conductivity of the contained medium. However, changes in measurements result from changes in internal conductivity and changes in the shape of the medium relative to the electrode positions. Failure to account for shape changes results in a conductivity image with significant artifacts. Previous work to address shape changes in EIT has shown that: a) theoretically, for an infinite number of electrodes, non-conformal changes in boundary shapes and electrode locations can be uniquely determined (Lionheart, 1998); and b) in some cases, conductivity and shape changes can be recovered using a combined image reconstruction model of both conductivity and shape changes (Soleimani *et al*, 2006). This work has shown that the shape change problem can be partially addressed. In this paper, we explore the limits of compensation for boundary movement in EIT, using three approaches: first, a theoretical model is developed to separate a deformation vector field into conformal and non-conformal components, from which the reconstruction limits may be determined; next, finite element models are constructed from which EIT measurements are simulated; finally, an experimental phantom is constructed using a deformable gasket and stainless steel electrodes in a saline medium, from which boundary deformation measurements are acquired.**

I. Introduction

In medical Electrical Impedance Tomography (EIT), it has long been suspected that errors in the knowledge of the boundary shape are an important factor in the inaccuracy of reconstruction. This effect is most important in chest EIT where the chest shape deforms as the patient breathes and changes posture[2][3].

In general terms, if a distortion is applied to a domain in two or three dimensional space, the assumed isotropy of the conductivity distribution is not preserved.[4] If the conductivity is assumed to be isotropic, the boundary voltage and current data on the distorted domain will generally not be consistent with an isotropic conductivity. This means that in the isotropic case, the boundary data contains information about both the conductivity and the boundary shape.

However, not all distortions lead to an anisotropic conductivity containing this additional information. The exception is exactly the distortions that are conformal maps. In two dimensional space, there are an infinite number of conformal maps, whereas in three dimensions there is only a finite set of conformal maps, the Möbius transformations.

In practical EIT, we would not usually want to use the electrical measurement to recover the boundary shape, as one could employ mechanical or optical measurement devices to determine the external shape of the body and the position of the electrodes. In the case of the chest, however, the boundary shape changes with breathing, so it is desirable to correct the boundary shape using the EIT data so that a consistent isotropic conductivity can be fitted to the data. This should result in a distorted image due to the anisotropic nature of chest muscle, yet still preserve useful features of the lungs.

In this paper, we explore the ability and limits of EIT to resolve conductivity changes and reject boundary distortion. First, we show that the theoretical results given in [4] still hold in the case of a finite number of electrodes and a finite element discretization of the forward problem. Our example simulations in two dimensions, using a linearization of the forward problem, suggest that the boundary shape and electrode positions can be recovered up to an infinitesimal conformal map. This provides an adequate and necessary correction for acceptable reconstruction of the conductivity.

In order to validate these results experimentally, we develop a deformable phantom from which we test the theoretical and simulated results.

II. Mathematical Background: Conformal Vector Fields

The linearization of a distortion of the domain is simply the addition of a vector field $\mathbf{V}$ to each point. If the distortions are all conformal mappings (that is, preserve the angle between vectors) then $\mathbf{V}$ is what is known classically as an *infinitesimal conformal motion*, *conformal Killing field*, or more simply a conformal vector field.

Assuming sufficient smoothness, $\mathbf{V}$ is a conformal vector field if and only if the conformal Killing field equation is satisfied. (Eq. 1.)

$$\frac{\partial V_i}{\partial x_j} + \frac{\partial V_j}{\partial x_i} = (\mathrm{div}\mathbf{V})\delta_{ij} \quad (1)$$

In two dimensions this reduces to

$$\frac{\partial V_1}{\partial x_1} - \frac{\partial V_2}{\partial x_2} = 0 \text{ and } \frac{\partial V_1}{\partial x_2} + \frac{\partial V_2}{\partial x_1} = 0 \quad (2)$$

which are the Cauchy-Riemann equations, hence in two dimensions $\mathbf{V}$ is a conformal vector field if and only if $V_1 + \mathrm{i}V_2$ is complex analytic as a function of $x + \mathrm{i}y$

As V_1 and V_2 are harmonic conjugate functions, they both satisfy Laplace's equation and at the boundary the tangential component of the gradient of V_1 is equal to the normal component of the gradient of V_2. Thus, V_1 can be specified arbitrarily on the boundary, and its tangential derivative, dV_1/ds where s is arc length on the boundary, is determined. Thus, V_2 is the solution of a Neumann problem for Laplace's equation and is determined up to a constant. Constants added to V_1 and V_2 correspond to a translation, which we would not expect to find from EIT data.

In a Finite Element setting, the infinitesimal vector field becomes a vector that translates each vertex of the finite element mesh. The discretization of the conformal vector field is determined uniquely by its values at the vertices on the boundary.

III. Simulated Results

In order to explore the effect of reconstructing EIT images from media with conformal and non-conformal conductivity changes, we constructed 2D simulations using the EIDORS software [1]. Using a 576 element FEM filling the unit circle with 16 point electrodes and using adjacent stimulation and measurement, we simulated two distortion fields. Representing each boundary point by a complex $z = x + \mathrm{i}y$, the distortions were:

$$z \to \quad 0.99x + \mathrm{i}1.01y \quad \textit{Non-conformal} \quad (3)$$
$$z \to \quad z + 0.01z^2 \quad \textit{Conformal} \quad (4)$$

Additionally, one small conductive and one small non-conductive target were simulated.

Using the approach of Soleimani *et al* [5], we reconstructed the time-difference conductivity and movement images. An assumed movement to conductivity change parameter $\mu = 0.01$ was used. For comparison, an algorithm was used which assumes no boundary movement. Results are shown in Fig. 1. For the case of non-conformal movements, there are dramatic artifacts in the conductivity only reconstruction, and there is a clear benefit to movement reconstruction. In the case of conformal movements, no such benefit is seen, and the movement reconstruction is unable to detect movement.

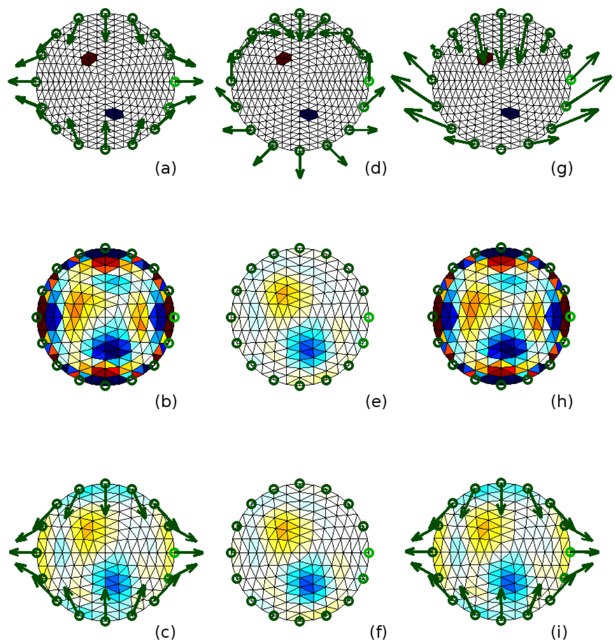

Fig. 1 Images reconstructed from three different movement patterns, illustrating that conformal distortion fields cannot be distinguished from conductivity changes. *Left (a), (b), (c):* Non-conformal Distortion field $z \to 0.99x + \mathrm{i}1.01y$. *Middle (d), (e), (f):* Conformal Distortion field $z \to z + 0.01z^2$. *Right (g), (h), (i):* Combined Conformal and Non-conformal Distortion field. *Top (a), (d), (g):* Simulation movement and conductivity change pattern. *Middle (b), (e), (h):* Reconstruction assuming only conductivity change. *Bottom (c), (f), (i):* Reconstruction of conductivity change and movement. Green arrows indicate electrode movement ($40\times$ exaggeration).

IV. Experimental Data: Phantom

In the following, we describe the deformable phantom used to take EIT measurements for comparison with simulated results of the previous section.

A. Construction

The phantom is constructed of a sponge rubber plumbing gasket placed in a shallow pan. The gasket forms a thick rubber ring that is easily compressed yet rigid enough to return to its original shape easily.

Sixteen electrodes were constructed from stainless-steel wire pressed into the gasket, then looped over the edge of the gasket such that they lie along the inner wall of the gasket in a vertical orientation. An additional stainless-steel electrode placed roughly in the geometric center of the gasket forms the ground connection. A shallow layer of saline solution is employed to limit conductivity in the vertical direction, thereby presenting an approximately two-dimensional section in the experimental measurements. The electrodes are each wired to a terminal bolted to the plastic pan providing a good connection to the EIT system. (Fig. 2.)

The thickness of the gasket allows the electrodes to be securely attached to the phantom as it is deformed. The thickness of the gasket also provides electrical insulation between the saline solution inside and outside the gasket.

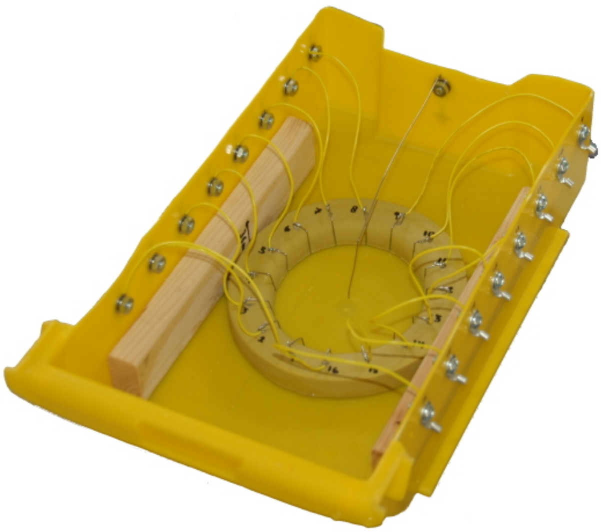

Fig. 2 Photograph of phantom built from a rubber gasket and stainless steel electrodes. The yellow dish is filled with saline.

B. Method

A 16 electrode Goë-MF II EIT system (Viasys Healthcare, Höchberg, Germany) was used for taking measurements from the deformable phantom. The phantom was submerged in a saline bath (0.68% NaCl salinity) such that the bottom of the ring was in contact with the bottom of the container, and the top of the ring broke the surface, providing insulation between the inside and outside of the ring. Salinity was set such that a nominal electrical impedance of 250Ω was measured between adjacent electrodes.

C. Deformations

Measurements were taken with the phantom in

- an approximately circular (relaxed) arrangement,
- with a side-to-side compression from two points, and
- with the ring under three points of compression. (Fig. 3.)

For each of these deformations measurements were obtained with

- a conductive target,
- a nonconductive target, and
- no target.

An iron cylinder with a diameter of 6mm was used as the conductive target while a glass cylinder of 42mm was used for the nonconductive target.

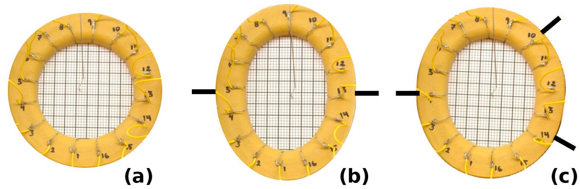

Fig. 3 Compressions: none (a), 2 points (b), 3 points (c)

D. Electrode Displacements

The true physical displacements of the electrodes were found by taking a digital photograph from above the phantom. A piece of graph paper was placed under the phantom, taped to the bottom of the pan. The locations of the electrodes were measured from the photograph, in pixels, and then normalized based on the known graph paper grid size.

V. Experimental Data: FEM Simulations

With the EIDORS software[1], the experimental EIT data measured from the phantom was used in reconstructing 2D images of the targets. An initial model consisting of a 256 element FEM filling the unit circle with 16 point electrodes was constructed. The mean of a sequence of data frames measured from the uncompressed phantom was used as an image prior.

Figure 4 shows the reconstructed images. Reconstructions under compression that did not account for the movement of electrodes displayed significant artifacts in the reconstructed image, particularly around the boundary. When accounting for conductivity and movement changes together the algorithm performed well (based on visual inspection) in estimating electrode movements as well as significantly reducing the image artifacts around the FEM boundary.

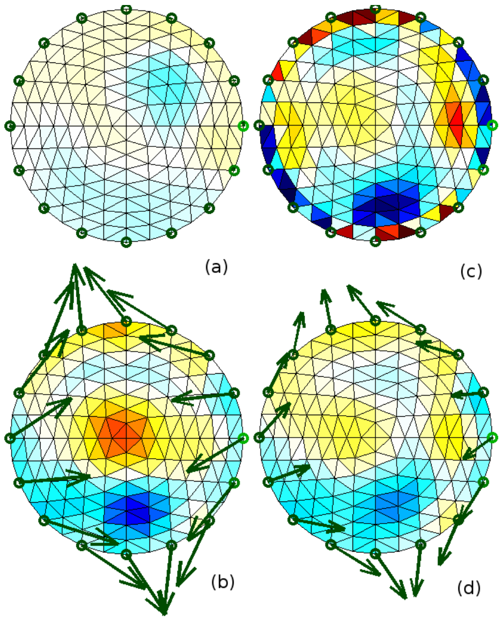

F ig. 4 Images reconstructed from experimental data. *Top Left, (a):* Reconstruction of no compression scenario. *Top Right, (c):* Reconstruction of 2-point compression assuming only conductivity change. (3-point compressions look very similar.) *Bottom:* Reconstruction of movement with 2-point *(b)* and 3-point *(d)* compressions. (Movement reconstruction with and without conductivity change resulted in similar images.) Green arrows indicate electrode movement (2× exaggeration).

VI. Discussion and Conclusion

This paper describes conformal and non-conformal vector fields and develops their application to electrode movement and boundary distortion in Electrical Impedance Tomography (EIT). Results, both in simulation and with experimental data, suggest that, with non-conformal mappings, electrode movement and boundary distortions can be reconstructed based on conductivity changes alone, reducing image artifacts in the process.

A limitation of this method is that the body is assumed to be isotropic. While this is a reasonable approximation for the lung, it it not true of muscle tissue or flowing blood. The effect of parts of the domain being anisotropic, possibly in a predictable orientation, is an interesting topic for further investigation.

This study was based on a linear approximation of the dependence of the transfer impedance data on both the conductivity and shape. Most in vivo EIT studies assume a linear approximation and typically reconstruct time or frequency difference images even though the forward problem is non-linear.

One reason given that a non-linear forward solution gives improved images on in vitro tank data but fails to deliver an improvement on in vivo reconstruction is that the errors caused by an inaccurate knowledge of boundary shape are greater than the error in using a linear approximation. This work holds out the hope that, with the correction of the boundary shape and electrode positions, using the EIT data will be sufficient for non-linear and accurate absolute EIT reconstruction of clinical data.

Acknowledgment

This work was supported by a grant from NSERC Canada.

References

1. Adler A, Lionheart WRB (2006) "Uses and abuses of EIDORS: An extensible software base for EIT." *Physiol. Meas.* 27 S25–S42
2. Adler A Guardo R and Berthiaume Y (1996) "Impedance imaging of lung ventilation: Do we need to account for chest expansion?" *IEEE Trans. Biomed. Eng.* 43 414–20
3. Coulombe N Gagnon H Marquis F Skrobik Y and Guardo R (2005) "A parametric model of the relationship between EIT and total lung volume" *Physiol. Meas.* 26 401–11
4. Lionheart WRB (1998) "Boundary Shape and Electrical Impedance Tomography" *Inverse Problems* 14 139–47
5. Soleimani M Gómez-Laberge C Adler A (2006) "Imaging of conductivity changes and electrode movement in EIT" *Physiol. Meas.* 27 S103–S113

Address of the corresponding author:
Author: Alistair Boyle
Institute: Carleton University
Street: 1125 Colonel By Drive
City: Ottawa
Country: Canada
Email: boyle@sce.carleton.ca